

Molecular Conformations of the Polymorphic Forms of Cimetidine from ^{13}C Solid-State NMR Distance and Angle Measurements

David A. Middleton,^{*,†} Cecile S. Le Duff,[‡] Xin Peng,[§] David G. Reid,[‡] and David Saunders[§]

Contribution from the Department of Biochemistry, University of Oxford, South Parks Road, Oxford OX1 3QU, U.K., Department of Analytical Sciences, SmithKline Beecham Pharmaceuticals, The Frythe, Welwyn, Hertfordshire AL6 9AR, U.K., and Department of Radiochemistry, SmithKline Beecham Pharmaceuticals, 709 Swedeland Road, King of Prussia, Pennsylvania 19406

Received August 23, 1999. Revised Manuscript Received November 18, 1999

Abstract: The polymorphic drug compound cimetidine, a histamine H_2 receptor antagonist, was synthesized containing sites of ^{13}C enrichment at the imidazolium methine carbon C2 and at the guanidinium methyl carbon C16. The structures of four crystalline forms of double ^{13}C -labeled cimetidine, three anhydrides (A, B, and C) and a monohydrate (M1), were examined using ^{13}C cross polarization magic angle spinning (CP-MAS) NMR methods. Rotational resonance magnetization exchange curves obtained for forms A and M1 were consistent with C2–C16 interatomic distances of 3.78 and 3.82 Å as measured from their crystal structures. Exchange curves for forms B and C, for which crystal structures have not been obtained, indicated that in both cases the C2–C16 interatomic distance lies between 5.2 and 5.8 Å, suggesting that cimetidine adopts a partially extended conformation in these forms. In addition, double quantum heteronuclear local field (2Q-HLF) NMR was used to determine the relative orientations of the ^{13}C –H bonds at the two ^{13}C -labeled sites. The experimental data were consistent with the known geometry of forms A and M1 and, in the case of form C, with a limited number of possible structures. Energetically favorable molecular conformations of form C, which were in agreement with the distance and angle measurements, fell into just six distinct clusters. These results demonstrate the feasibility of determining the complete solid-state structures of pharmaceutical compounds, and other materials not amenable to crystallography, using CP-MAS NMR combined with a minimal isotope labeling strategy.

Introduction

Many structurally diverse organic compounds can be induced to adopt two or more crystallographically distinct forms by varying the crystallization conditions.^{1,2} This phenomenon, known as polymorphism, has important implications for industries involved in the production of small organic molecules, since different crystalline forms of chemically equivalent materials can exhibit quite distinct physical properties.^{3,4} The pharmaceutical industry, for one, is acutely aware of the potential problems of structural polymorphism, which can have a profound effect on the dissolution rates, bioavailability, and ease of formulation of drug compounds,^{5,6} as well as raising issues of commercial exclusivity. In response to these concerns, there has been much effort toward developing techniques to identify, characterize, and predict novel crystalline forms of compounds.^{7–9}

There are now a number of strategies that use known physical and chemical features of organic molecules to predict their crystal structures and help assess the likelihood of compounds adopting more than one crystal form.^{10,11} Such methods include semi-empirical or sophisticated computational approaches using Monte Carlo simulated annealing procedures or molecular dynamics simulations.^{12–14} Their success rate tends to diminish with increasing molecular complexity, and also suffers in cases of molecules containing halogen atoms or unusual functionalities, but improvements are continually being made as more is learned about the molecular interactions that take place during crystal formation.

Determining the crystal structures of polymorphic compounds is a key step in validating these predictive computational methods. As the diversity of available crystal structures increases, so does our understanding of the intramolecular and intermolecular forces that affect molecular packing in general and influence structural polymorphism. Unfortunately, X-ray analysis is hampered in the 20% or more of cases in which

* Corresponding author. Telephone: +44 1865 275776. Fax: +44 1865 275234. E-mail: middleda@bioch.ox.ac.uk.

[†] University of Oxford.

[‡] Department of Analytical Sciences, SmithKline Beecham Pharmaceuticals, U.K..

[§] Department of Radiochemistry, SmithKline Beecham Pharmaceuticals, PA.

(1) Threlfal, T. L. *Analyst* **1995**, *120*, 2435.

(2) Haleblan, J.; McCrone, W. J. *J. Pharm. Sci.* **1969**, *58*, 911.

(3) Grunenberg, A. *Regelweiterbildungseminar Pharmazeutische Analytik*; Bonn, 1992; pp 1–8.

(4) Sussich, F.; Urbani, R.; Princivalle, F.; Cesàro, A. *J. Am. Chem. Soc.* **1998**, *120*, 7893.

(5) Haleblan, J. K. *J. Pharm. Sci.* **1975**, *64*, 1269–88.

(6) Byrn, S.; Pfeiffer, R.; Ganey, M.; Hoiberg, C.; Poochikian, G. *Pharm. Res.* **1995**, *12*, 945–54.

(7) Saindon, P. J.; Cauchon, N. S.; Sutton, P. A.; Chang, C.-J.; Peck, G. E., Byrn, S. R. *Pharm. Res.* **1993**, *10*, 197–203.

(8) Ripmeester, J. A. *Chem. Phys. Lett.* **1980**, *74*, 536–8.

(9) Byrn, S. R.; Gray, G.; Pfeiffer, R. R.; Frye, J. J. *J. Pharm. Sci.* **1985**, *74*, 565–8.

(10) Desiraju, G. R. *Science* **1997**, *278*, 404.

(11) Hanessian, S.; Simard, M.; Roelans, S. *J. Am. Chem. Soc.* **1995**, *117*, 7630.

(12) Gavezzotti, A. *Acc. Chem. Res.* **1994**, *27*, 309.

(13) Aakeröy, C. B.; Nieuwenhuyzen, M.; Price, S. L. *J. Am. Chem. Soc.* **1998**, *120*, 8986.

(14) Karfunkel, H.; Gdanitz, R. *J. J. Comput. Chem.* **1992**, *13*, 1171.

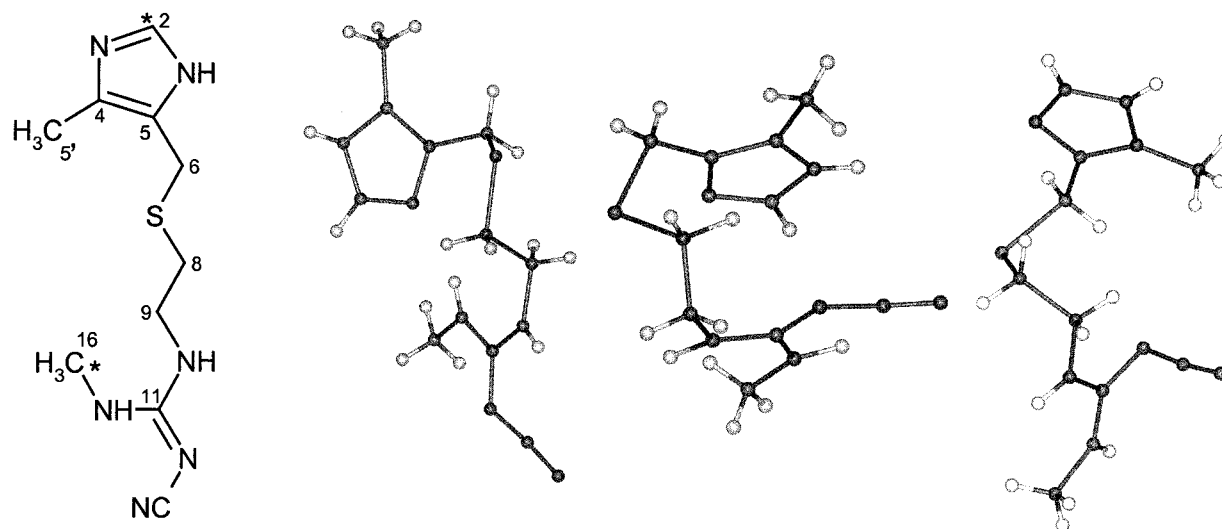


Figure 1. (A) Chemical structure and numbering system for cimetidine. (B) The molecular conformations in the crystallographic unit cell of the cimetidine anhydrate forms A (left) and D (middle), and the monohydrate M1 (right), as determined by X-ray diffraction. Crystal coordinates were taken from the Cambridge Structural Database, and the structures are published in refs 18 and 19.

organic compounds do not readily form diffracting crystals, and consequently the structures of some forms of a polymorphic compound may be known, while those of other forms remain intractable.¹⁵ An example is the histamine H₂ receptor antagonist, cimetidine (*N*-cyano-*N'*-methyl-*N''*-[2-[[5-methyl-1H-imidazol-4-yl]thio]ethyl] guanidine), one of the first documented cases of a polymorphic drug substance (Figure 1A).^{16,17} Cimetidine exists in four main stable anhydrate forms, A, B, C, and D, and a monohydrate M1. The crystal structures of forms A, D, and M1 have been solved^{18,19} (Figure 1B), but diffracting crystals of two of the anhydrous forms, B and C, have so far proved difficult to prepare, and crystal structures have not been obtained.

Although there are no comprehensive alternatives to X-ray crystallography for determining the structure and arrangement of organic compounds in a crystal lattice, recent advances in solid-state NMR spectroscopy promise to realize the prospect of determining the molecular conformations of compounds in the unit cell.^{7,20} A combination of cross polarization, proton decoupling, and magic angle spinning (CP-MAS) has enabled high-resolution spectra to be obtained from polycrystalline materials,^{8,21} providing a method for identifying and characterizing different forms of organic compounds including formulated pharmaceuticals.^{8,22,23} When combined with isotope labeling, with ¹³C and ¹⁵N, for example, advanced CP-MAS techniques are able to provide structural information on polycrystalline solids by measuring aspects of molecular geometry.^{24,25} The most successful and widely used of these techniques, rotational resonance²⁶ and REDOR,²⁷ have been used to measure precise through-space distances between pairs of labels in organic solids

and biological semi-solid materials. Their main disadvantage is that only a very limited amount of information—a single inter atomic distance from a spin-pair—is obtained, and determining the complete structure of a molecule may require synthesis of several compounds with pairs of labels at different sites. Two-dimensional (2D) CP-MAS NMR can increase the amount of information in a single experiment by identifying networks of connectivities between spins in multiple or uniformly isotope-labeled compounds, but multi-dimensional methods have so far proved more useful for resonance assignments than for providing precise structural information.^{20,28,29} The R2TR experiment of Takegoshi and co-workers³⁰ promises to be a feasible method for determining structures of multiple-labeled solids, but the problem remains that synthetic procedures for introducing many ¹³C or ¹⁵N sites into a molecule may not be available or are too expensive to be feasible.

This paper describes a novel strategy that combines ¹³C CP-MAS distance measurements with estimates of C–H bond orientations to examine the molecular conformations in different crystal forms of cimetidine. CP-MAS methods have recently come to the forefront which directly determine N–C–N or H–C–C–H torsion angles for compounds containing four directly bonded spins,^{31,32} such as in the side chain of retinal in bovine rhodopsin.³³ Here, cimetidine was synthesized with ¹³C labels placed at each end of the molecule, at imidazolium carbon C2 and guanidinium carbon C16 (Figure 1A), from small, inexpensive ¹³C precursors as part of the commercial synthetic

(15) Docherty, R. *J. Am. Chem. Soc.* **1997**, *119*, 1767.

(16) Brimblecombe, R. W.; Duncan, W. A. M.; Durant, G. J.; Emmett, J. C.; Ganellin, C. R.; Parsons, M. E. *J. Int. Med. Res.* **1975**, *3*, 86–92.

(17) Hegedüs, B.; Görög, S. *J. Pharm. Biomed. Anal.* **1985**, *3*, 303.

(18) Shibata, M.; Kokubo, H.; Morimoto, K.; Morisaka, K.; Ishida, T.; Inoue, M. *J. Pharm. Sci.* **1983**, *72*, 1436.

(19) Prodić-Kojic, B.; Kajfes, F.; Belin, B.; Toso, R.; Sunjic, V. *Gazz. Chim. Ital.* **1979**, *109*, 535.

(20) Zell, M. T.; Padden, B. E.; Grant, D. J. W.; Chapeau, M.-C.; Prakash, I.; Munson, E. J. *J. Am. Chem. Soc.* **1999**, *121*, 1372.

(21) Smith, J.; MacNamara, E.; Raftery, D.; Borchardt, T.; Byrn, S. J. *Am. Chem. Soc.* **1998**, *120*, 11710.

(22) Chang, C.; Diaz, L. E.; Morin, F.; Grant, D. *Magn. Res. Chem.* **1986**, *24*, 768.

(23) Middleton, D. A.; Le Duff, C. S.; Berst, F.; Reid, D. G. *J. Pharm. Sci.* **1997**, *86*, 1400.

(24) Marshall, G. R.; Beusen, D. D.; Kociolek, K.; Redlinski, A. S.; Leplawy, M. L.; Pan, Y.; Schaefer, J. *J. Am. Chem. Soc.* **1990**, *112*, 963.

(25) Nomura, K.; Takegoshi, K.; Terao, T.; Uchida, K.; Kainosho, M. *J. Am. Chem. Soc.* **1999**, *121*, 4064.

(26) Raleigh, D. P.; Levitt, M. H.; Griffin, R. G. *Chem. Phys. Lett.* **1988**, *146*, 71.

(27) Gullion, T.; Schaefer, J. *J. Magn. Reson.* **1989**, *81*, 196.

(28) Sun-B. Q.; Costa, P. R.; Koscioko, D.; Lansbury, P. T.; Griffin, R. G., *J. Chem. Phys.* **1995**, *102*, 702.

(29) Sun, B. Q.; Rienstra, C. M.; Costa, P. R.; Williamson, J. R.; Griffin, R. G. *J. Am. Chem. Soc.* **1997**, *119*, 8540.

(30) Takegoshi, K.; Nomura, K.; Terao, T. *J. Magn. Reson.* **1997**, *127*, 206.

(31) Feng, X.; Lee, Y. K.; Sandström, D.; Edén, M.; Maisel, H.; Sebald, A.; Levitt, M. H. *Chem. Phys. Lett.* **1996**, *257*, 314.

(32) Costa, P. R.; Gross, J. D.; Hong, M.; Griffin, R. G. *Chem. Phys. Lett.* **1997**, *280*, 95.

(33) Feng, X.; Verdegem, P. J. E.; Lee, Y. K.; Sandström, D.; Edén, M.; Bovee-Geurts, P.; de Grip, W. J.; Lugtenburg, J.; de Groot, H. J. M.; Levitt, M. H. *J. Am. Chem. Soc.* **1997**, *119*, 6853.

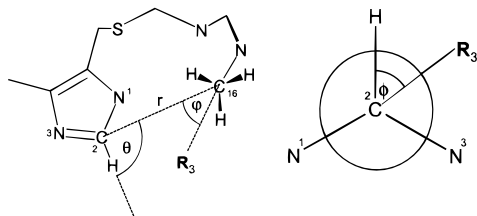


Figure 2. Illustrations of some geometric terms describing the molecular conformation of cimetidine. Left: the through-space distance between C2 and C16 is denoted r , the angle between the C2–H bond and the C2–C16 inter-nuclear vector is denoted θ , and φ defines the angle between the C16–C2 internuclear vector and the 3-fold rotation axis R_3 . Right: the effective torsion angle H–C2–C16– R_3 is denoted ϕ .

route. The aim of the work was to maximize the amount of structural information that could be obtained by CP-MAS NMR from just two ^{13}C labels and thereby determine the molecular conformations of cimetidine in the structurally undefined forms, B and C, economically and without recourse to crystallography. The NMR strategy was as follows. First, the different crystalline forms were identified from their natural abundance ^{13}C CP-MAS spectra as described in a previous report.²³ Second, rotational resonance magnetization NMR was used to measure the C2–C16 interatomic distance in each form (Figure 1C). Third, an experiment reported by Feng et al.,³¹ double quantum heteronuclear local field (2Q-HLF) NMR, was used to determine the angles (φ , θ , and ϕ) defining the relative orientations of the C–H bonds at the ^{13}C -labeled sites (Figure 2). Finally, the distance and angle measurements were used as restraints for preliminary modeling of the solid-state molecular conformations of cimetidine. The validity of this approach was first assessed by comparing experimental results with the response predicted for the known molecular geometry of cimetidine forms A and M1, before continuing to examine the structures of forms B and C.

Methods and Materials

Synthesis of [$^{13}\text{C}_2$]cimetidine. Double ^{13}C -labeled cimetidine (Figure 1A) was synthesized using a modification of a previous route.³⁴ Briefly, potassium [^{13}C]thiocyanate was prepared from commercially available potassium [^{13}C]cyanide and condensed with ethyl 2-aminoacetate hydrochloride to give [2- ^{13}C]4-ethylaceto-5-methyl-2-thioimidazole. All remaining steps were carried out as described in ref 34, except that [^{13}C]methylamine hydrochloride was substituted for natural abundance isotope methylamine in the final reaction to afford pure [$^{13}\text{C}_2$]cimetidine after normal-phase gravity column purification.

Preparation of [$^{13}\text{C}_2$]cimetidine Forms. Three forms of cimetidine anhydrate (A, B, and C) and the monohydrate form (M1) were prepared as described previously.²³ Success in recrystallizing cimetidine into each of the desired forms was erratic, and the presence of each pure form was ascertained from their ^{13}C CP-MAS NMR spectra.²³ Forms B and M1 were particularly unstable, converting to form A over a period of hours to days. Samples of each form were packed into MAS rotors for NMR analysis without grinding or application of excess pressure to avoid interconversion between forms.

NMR Spectroscopy. Spectra were acquired at 8.4 T on a Bruker AMX360WB spectrometer or at 4.7 T on a Chemagnetics CMX-200 system interfaced to Bruker temperature control and spinning units. All experiments were performed using Bruker double resonance MAS probes fitted with 7 or 4 mm spinning modules. Samples of forms A, B, C, and M1 were contained in zirconia MAS rotors fitted with Kel-F caps and were spun at MAS frequencies of between 3 and 11 kHz at ambient temperature.

(34) Villiani, A. J.; Petka, L.; Blackburn, D. W.; Saunders, D.; White, G. R.; Winster, J. *J. Labelled Compd. Radiopharm.* **1989**, *12*, 1395–1402.

Hartmann–Hahn cross polarization from protons to carbon was carried out at a proton nutation frequency of 83 kHz over a contact time of 1.6 ms. The two-pulse, phase-modulated (TPPM) decoupling sequence of Bennet and co-workers³⁵ was used for proton decoupling, also at a field of 83 kHz. Free induction decays were digitized into 1K of data points and Fourier-transformed into 4K points after applying 10 Hz exponential line-broadening. Zeeman magnetization exchange experiments at first order ($n = 1$) rotational resonance (R^2) were carried out using the standard experiment described elsewhere.³⁶ First-order R^2 for all forms of cimetidine was achieved at a spinning frequency ($\omega_r/2\pi$) of about 9.6 kHz. Nonselective 90° pulse lengths of 4 μs were applied at the ^{13}C frequency, and selective inversion of ^{13}C spins was achieved using a DANTE pulse train. Magnetization exchange between ^{13}C spins was followed over mixing times ranging from 1 to 20 ms.

The 2Q-HLF NMR experiment was carried out as described by Feng et al.³¹ at a spinning frequency of 3 kHz. After cross polarization, ^{13}C magnetization was returned to the z axis by a 4- μs 90° pulse and converted into double quantum (2Q) coherence using the C7 excitation sequence,³⁷ in which the B_1 field was adjusted to 21 kHz ($7\omega_r/2\pi$) over a 2Q excitation time of 2 ms. The 2Q coherence was then allowed to evolve for a constant interval τ_1 , the rotor period, during which the ^1H – ^1H dipolar couplings were suppressed for a time t_1 ($t_1 \geq \tau_1$) using the homonuclear decoupling sequence MREV-8,³⁸ before reverting to standard broad-band ^{13}C – ^1H decoupling. The ^1H field was increased to 83 kHz throughout τ_1 and then decreased to 63 kHz for the remainder of the pulse sequence. The modulated 2Q coherences were converted back into observable magnetization by a second C7 sequence of 2 ms followed by a nonselective 90° pulse at the ^{13}C frequency. FIDs were digitized into 512 points, and 2Q filtration was carried out as described previously, by phase-shifting the second C7 sequence and combining the digitized signal with a series of complex linear factors. A set of 17 experiments were carried out for each [$^{13}\text{C}_2$]cimetidine form, in which the ^1H – ^1H decoupling time t_1 was incremented from zero to τ_1 by 16 equal time periods. The evolution of 2Q coherence under the influence of ^1H homonuclear decoupling is observed as the NMR signal amplitude at each value of t_1 and is compared with numerical simulations of the experimental amplitudes to determine the angles between the C–H bond vectors.

Results and Discussion

NMR Spectra of Cimetidine. Previous work showed that four of the pure cimetidine anhydrate forms, A, B, C, and D, and the monohydrate form M1, could be identified unambiguously from their ^{13}C CP-MAS spectra.²³ Spectra of the forms A, C, D, and M1 contained one peak for each carbon atom and indicated that the crystallographic asymmetric unit consisted of a single molecule. By contrast, the spectrum of form B exhibited two resolved peaks for most of the carbon atoms, indicating that at least two crystallographically nonequivalent molecules occupied the unit cell.

The NMR spectra of [$^{13}\text{C}_2$]cimetidine containing an 8-fold molar excess of labeled compound [$^{13}\text{C}_2$]cimetidine are dominated by resonances from the ^{13}C -enriched imidazolium carbon C2 (~ 37 ppm) and the guanidinium N -methyl carbon C16 (~ 135 ppm). The isotropic chemical shift values for C2 and C16 in each form are summarized in Table 1 and full spectra of forms B and C at 8.4 T are shown in Figure 3. Closer inspection of the spectra of the five cimetidine forms revealed that the line shapes of the two peaks were slightly asymmetric. Spectra of the same forms obtained at a lower static field of 4.7 T (Figure 3, inset) showed a clear splitting of the low-field and high-

(35) Bennet, A. E.; Rienstra, C. M.; Auger, M.; Lakshmi, V.; Griffin, R. G. *J. Chem. Phys.* **1995**, *103*, 6951.

(36) Peersen, O. B.; Groesbeek, M.; Aimoto, S.; Smith, S. O. *J. Am. Chem. Soc.* **1995**, *117*, 7228.

(37) Lee, Y. K.; Kurur, N. D.; Helmle, M.; Johannessen, O. G.; Nielsen, N. C.; Levitt, M. H. *Chem. Phys. Lett.* **1995**, *242*, 219.

(38) Mansfield, P. *J. Phys.* **1971**, *C4*, 1444.

Table 1. NMR Spectroscopic Parameters for the Anhydrate (A, B, C, and D) and Monohydrate (M1) Forms of Cimetidine, and a Summary of the Measured Distances and Angles Related to the Three-Dimensional Structure of Cimetidine in the Crystallographic Unit Cell^a

cimetidine form	¹³ C chemical shift (ppm)		C2–C16 distance <i>r</i> (Å)	C(2)H–C(16)H ₃ angles ^a (deg)		
	C16 ^c	C2		φ	θ	ϕ
A ^b	27.9	135.9	3.8	108	62	43
B ^c	27.6	134.8	5.5 ± 0.3	0–70, 110–180	0–75, 105–180	0–75, 105–180
C ^c	27.4	132.4	5.5 ± 0.3	0–20, 160–180	30–150	30–150
D ^b	28.9	133.1	9.1	129	141	8
M1 ^b	28.6	135.1	3.8	114	70	63

^a The definitions of *r*, φ , θ , and ϕ are given in Figure 2. ^b Distances and angles measured from the crystal structures deposited in the Cambridge Structural Database (and references therein). ^c Distances obtained by rotational resonance magnetization exchange measurements, and angles obtained from 2Q-HLF amplitudes.

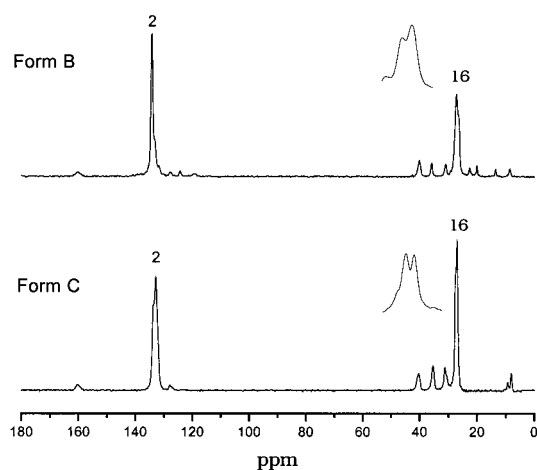


Figure 3. Proton-decoupled, ¹³C CP-MAS NMR spectra of [¹³C₂]-cimetidine diluted with an 8-fold molar excess of natural abundance cimetidine and crystallized from water as form B (top) and form C (bottom). The insets highlight the 80–100 Hz splitting of the peaks from the guanidinium carbon C16.

field peaks into a poorly resolved asymmetric doublet separated by about 80 Hz. Similar features were previously observed in natural abundance ¹³C spectra of cimetidine,²⁴ but without isotope labeling it was not clear if the peaks were split or were actually composed of two overlapping resonances from chemically unique carbons. Here, isotope labeling confirmed that peak splitting originated from the residual dipolar coupling between ¹³C and directly bonded quadrupolar ¹⁴N, which cannot be eliminated by sample rotation.³⁹

Strategy for Cimetidine Structure Determination. The strategy for determining the molecular conformations of the cimetidine crystal forms B and C was based on two NMR experiments, which rely on through-space interactions between the ¹³C isotope labels. Rotational resonance NMR was used to determine the C2–C16 interatomic distance in each cimetidine form by reintroducing the weak ¹³C dipole–dipole interaction (which is removed by sample spinning under normal conditions) and observing Zeeman magnetization exchange between the recoupled spins over a series of mixing intervals. To attain first-order (*n* = 1) rotational resonance the MAS frequency was

(39) Opella, S. J.; Frey, M. H.; Cross, T. A. *J. Am. Chem. Soc.* **1979**, *101*, 5856. Hexem, J. G.; Frey, M. H.; Opella, S. J. *J. Chem. Phys.* **1982**, *77*, 3847. Harris, R. K.; Olivieri, A. C. *Prog. Nucl. Magn. Reson. Spectrosc.* **1992**, *24*, 435.

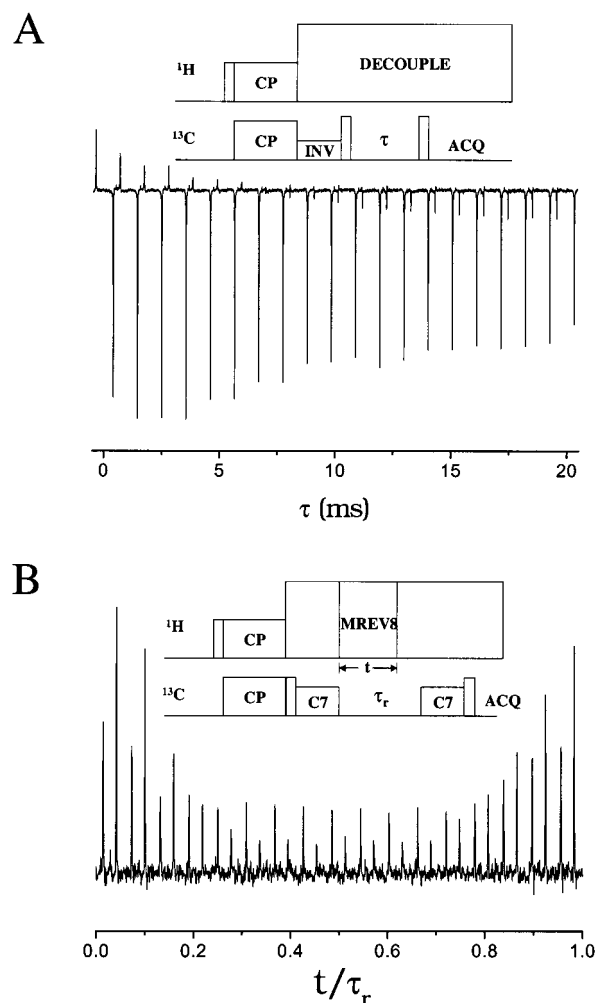


Figure 4. (A) A series of rotational resonance NMR spectra (at 8.4 T) of [¹³C₂]-cimetidine (form A) diluted 8-fold with unlabeled cimetidine. The peak intensities over a series of mixing times are related to Zeeman magnetization exchange at first-order rotational resonance. (B) A series of ¹³C 2Q-HLF NMR spectra (at 4.7 T) of [¹³C₂]-cimetidine (form A) recorded by varying the duration of proton homonuclear decoupling from zero (left-hand spectrum) to 333 μs, one rotor period (right-hand spectrum). The insets illustrate pulse sequences for rotational resonance (A) and 2Q-HLF NMR (B).

adjusted to match the frequency separating the isotropic chemical shifts of C2 and C16, which was 9400s ± 300 Hz at 8.4 T. Spectra of cimetidine form A, collected over a series of mixing times at *n* = 1 rotational resonance, are shown in Figure 4A. The resonance line from C16 was selectively inverted to create opposite polarizations of the two ¹³C spins, and the decay of signal intensity with increasing mixing interval was ascribed in part to Zeeman magnetization exchange under the time-dependent homonuclear dipolar Hamiltonian. Numerical simulations of the combined C2 and C16 peak integral values at each mixing time were carried out to determine the distance-dependent dipole coupling constant *b*^{CC} (see next section).

In addition to the rotational resonance experiments, 2Q-HLF NMR was used to estimate the orientation of the imidazolium C–H bond relative to the guanidinium CH₃ group and thereby obtain additional constraints to define the molecular structure of forms B and C. The experiment determines the relative orientations of correlated proton-carbon fields by following the modulation of ¹³C double-quantum (2Q) coherences over one

sample rotation cycle under the influence of the fields generated by local protons. The procedure was carried out as follows. After excitation of 2Q coherences by a standard method,³⁸ the ¹³C transmitter was turned off for one rotor period (τ_R). Proton–proton interactions were removed during this period, first using the homonuclear decoupling sequence MREV-8,³⁹ which retains local ¹³C–¹H interactions, and then by broad band continuous wave irradiation, which eliminates both ¹H–¹H and ¹³C–¹H couplings. The 2Q coherence was converted to observable magnetization, and the FID was collected. In practice, a series of spectra were acquired in which the evolving 2Q coherences experienced local proton fields for an increasing length of time, by incrementing the duration (t) of the MREV-8 sequence from zero to τ_R (Figure 4B). Modulation of the C2 and C16 peak amplitudes over τ_R are sensitive to the relative orientation of the protons bonded to the two ¹³C-labeled sites, and numerical simulations of the amplitudes were performed to find the angles (φ , θ , and ϕ) relating the C–H bonds to a defined reference frame (Figure 1C).

Rotational resonance and 2Q-HLF NMR are sensitive to the magnitude of the ¹³C–¹³C dipolar coupling constant b^{CC} , which, in turn, is inversely proportional to the cube of the interatomic distance r^{CC} according to the relation⁴⁰

$$b^{IS} = -\left(\frac{\mu_0}{4\pi}\right) \frac{\gamma_I \gamma_S \hbar}{r_{IS}^3} \quad (1)$$

Hence, b^{CC} increases from 60 Hz in the case of ¹³C pairs separated by 5 Å to about 3000 Hz for a single bonded ¹³C pair. Coupling constants of less than 30 Hz are too small to be determined accurately from rotational resonance magnetization exchange curves and in practice distances between ¹³C atoms of up to 6.5 Å can be measured reliably (to ± 0.5 Å) by this technique, depending on the quality of the spectral data.³⁷ Similarly, the efficiency of double-quantum excitation by the C7 sequence diminishes with increasing interatomic distance. The experimental double-quantum filtering efficiency for directly bonded ¹³C atoms is about 50%, reducing to about 1% for ¹³C atoms separated by 5.5 Å. Virtually no 2Q transfer occurs at separations of 6 Å and above.

The C2–C16 interatomic distances measured from the available crystal structures of cimetidine are given in Table 1. Forms A and M1 adopt a “horseshoe” conformation in which the guanidinium proton internally hydrogen bonds to the imidazolium nitrogen, and C2 and C16 are separated by less than 4 Å (Figure 1B). This interatomic distance is well below the upper limit accessible to rotational resonance and 2Q-HLF NMR. Form D, however, exists in an extended configuration stabilized by intermolecular hydrogen bonds, and C2 and C16 are separated by 9.1 Å (Figure 1 and Table 1). This distance is outside the range accessible to the NMR methods, and therefore form D could not be examined spectroscopically. Since no structural information was available for cimetidine forms B and C, we had no prior indication of whether their molecular geometry was favorable for the NMR measurements, or whether, like form D, the C2–C16 separation was too large to give rise to a detectable response.

The final stage of the strategy was to combine the distance and angle measurements with a computational approach to determine the molecular conformations of the cimetidine forms B and C. The outcome of this exercise depended on whether

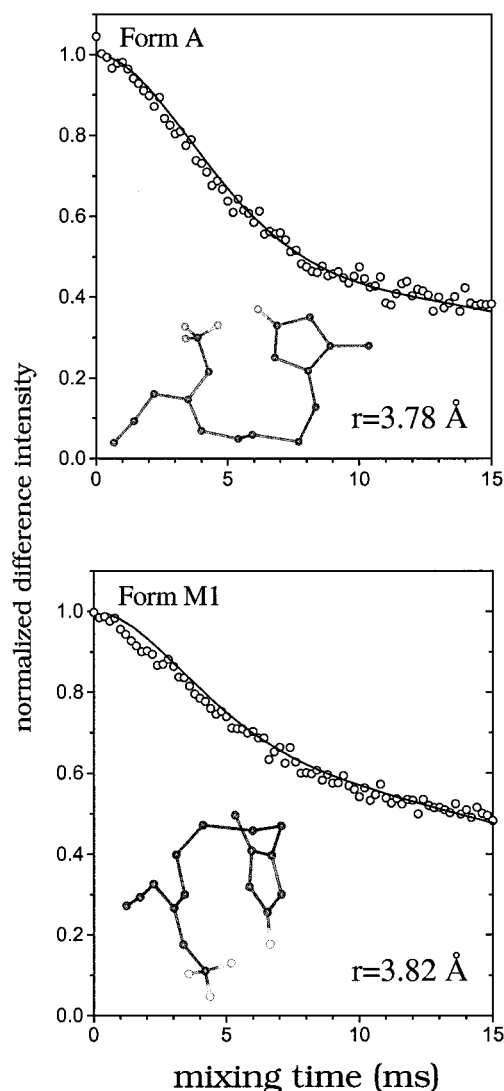


Figure 5. Magnetization exchange curves at first order ($n = 1$) rotational resonance for [¹³C₂]cimetidine crystallized as forms A (top) and M1 (bottom) with an 8-fold molar excess of unlabeled cimetidine. Open circles show the experimental data measured from the combined peak integrals for sites C2 and C16. Solid lines are numerical simulations calculated for the each distance r shown.

the experimental data could be interpreted unambiguously and on the number of energetically favorable cimetidine structures consistent with the distance and angle measurements.

Distance Measurements. Distances between nonequivalent pairs of ¹³C nuclei contained within the same molecule can be measured with high precision by rotational resonance NMR, provided they are not coupled to nonequivalent spins in neighboring molecules. Diluting [¹³C₂]cimetidine with an 8-fold molar excess of unlabeled material was sufficient to fully eliminate intermolecular couplings, but it was necessary to use difference spectroscopy to remove the natural abundance contribution to the peaks of interest before integration and analysis.

Zeeman magnetization exchange curves (corrected for natural abundance signal) for forms A and M1 of [¹³C₂]cimetidine at first order ($n = 1$) rotational resonance are shown in Figure 5, and Figure 6 shows curves obtained under similar conditions for forms B and C. Each point represents the mean of three experiments carried out under identical conditions; standard errors were very small (less than 5% of the mean) and are not

(40) See, for example: Ernst, R. R.; Bodenhausen, G.; Wokaun, A. *Principles of magnetic resonance in one and two dimensions*; Clarendon Press: Oxford, 1987.

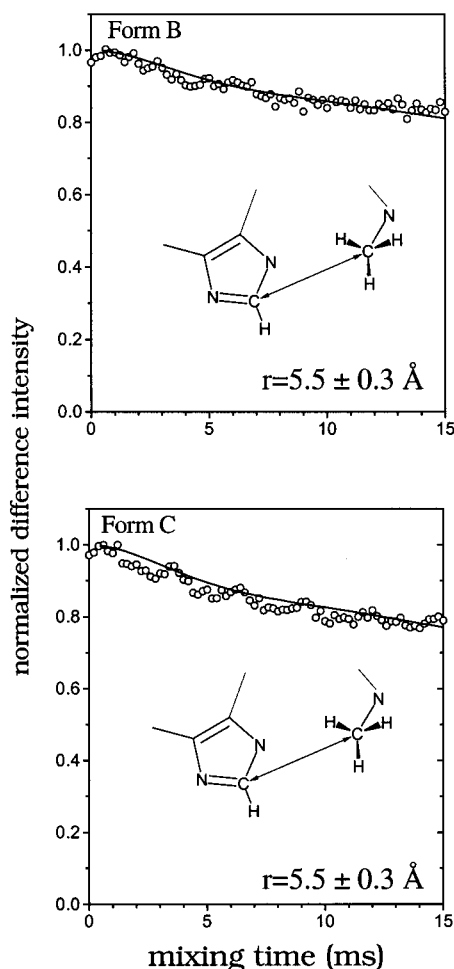


Figure 6. Magnetization exchange curves at first order ($n = 1$) rotational resonance for $[^{13}\text{C}_2]$ cimetidine crystallized as forms B (top) and C (bottom). Lines and symbols are as described for Figure 5.

shown. The numerical procedures described by Levitt et al.⁴¹ were used to simulate the experimental exchange curves and determine the C2–C16 interatomic distance for each cimetidine form. The numerical simulations require a number of input parameters. These include the homonuclear dipole coupling constant b^{CC} , the set of Euler angles (Ω_{PM}) defining the relative orientations of the C2 and C16 chemical shift tensors with respect to the inter-nuclear vector, and a damping factor, T_2^{ZQ} , known as the zero-quantum relaxation time.⁴² The relative orientations of chemical shift tensor elements are not known for cimetidine, but were estimated from values for ^{13}C nuclei in similar compounds. It was found, however, that varying the Euler angles, α_{PM} , β_{PM} , and γ_{PM} , had little effect on the appearance of the calculated curves at $n = 1$ rotational resonance because of the large separation of the isotropic chemical shifts for the two sites compared to their chemical shielding anisotropy. By contrast, the value of T_2^{ZQ} has a pronounced effect on the shape of the calculated exchange curves. The precise value of T_2^{ZQ} was uncertain, but was estimated from the sum of the spectral peak widths at half-height from C2 and C16 as described elsewhere.⁴²

Numerical simulations of the experimental data for each form were carried out as follows. Several curves were computed from

the unknown input parameters, b^{CC} , T_2^{ZQ} , or both, varied over acceptable ranges as predetermined from the spectral peak widths and the detection limits of the rotational resonance experiment. The calculated curves were compared with the experimental curves to find the combination of input parameter values producing the best fit to the data points as determined by χ^2 analysis. In the case of forms A and M1 (Figure 5), b^{CC} was calculated from the C2–C16 distance measured from the crystal structures and was kept constant, while T_2^{ZQ} was incremented within limits of ± 2 ms from the value measured from the peak widths. For each cimetidine form, the T_2^{ZQ} value producing the curve most closely fitting the experimental data was very close to the value obtained directly from the spectral peak widths.

The values of both b^{CC} and T_2^{ZQ} were not known in the case of forms B and C, and therefore both parameters were varied independently to generate a two-dimensional array of calculated curves, from which the closest fitting curves to the experimental data were selected (Figure 6). Because of the uncertainties in two parameters, χ^2 analysis gave a number of T_2^{ZQ} and b^{CC} combinations consistent with the experimental Zeeman exchange curves for forms B and C (Table 1). As before, the T_2^{ZQ} values were close to those predicted from the spectral peak widths, and b^{CC} values translated to identical C2–C16 distance ranges for both forms, 5.5 ± 0.3 Å for form B and 5.5 ± 0.3 Å for form C.

Measurements of Bond Orientations. The theory describing the evolution of double-quantum coherence under a local proton field of variable duration has so far been limited to the case of a fixed-geometry ^{13}C – ^1H pair double bonded through carbon.^{31,33} The theoretical treatment must, therefore, be adapted to take into account the specific case of $[^{13}\text{C}_2]$ cimetidine, with its remote and indirectly bonded ^{13}CH and $^{13}\text{CH}_3$ groups. Numerical simulations of the modulated 2Q amplitudes for a four-spin system of the type H_1 – C_1 – C_2 – H_2 over one cycle of sample rotation (e.g., Figure 4B) are derived from the MAS frequency-dependent proton dipolar fields, ω_{11}^{HC} , ω_{21}^{HC} , ω_{12}^{HC} , ω_{22}^{HC} . The terms ω_{11}^{HC} and ω_{22}^{HC} represent the high local fields experienced by each carbon nucleus from bonded protons, while ω_{21}^{HC} and ω_{12}^{HC} are cross-terms for the small fields at each carbon arising from the remote proton bonded to the adjacent carbon. Values of ω_{ij}^{HC} for a given molecular orientation in a powder sample, at time increments over a full rotor period, are related to the distance-dependent ^1H – $^{13}\text{C}_j$ dipolar coupling constants b_{ij}^{HC} and the relative orientations of the internuclear vectors, as³¹

$$\omega_{jk}^{\text{HC}} = \sum_{m',m} b_{jk}^{\text{HC}} D_{0m'}^2(\Omega_{\text{PM}}^{jk}) D_{m'm}^2(\Omega_{\text{MR}}) e^{(im\omega_r t)} d_{m0}^2(\beta_{\text{RL}}) \quad (2)$$

The set of Euler angles Ω_{PM} relate the C–H bond vectors to the molecular reference frame whose z -axis is the ^{13}C – ^{13}C internuclear distance vector (Figure 2) and are calculated from the fixed HCC bond angles and the HCCH torsion angle. The Euler angles Ω_{MR} relate the molecular reference frame to a rotor-fixed axis system. In the case of a methyl group rotating about its 3-fold axis rapidly with respect to the MAS rotational frequency, the time-averaged field $\bar{\omega}_{jk}^{\text{HC}}(t)$ from each single proton is given by

$$\bar{\omega}_{jk}^{\text{HC}}(t) = \frac{1}{N} \sum_{i=1}^N \omega_{jk}^{\text{HC}}(t, i) \quad (3)$$

(41) Levitt, M. H.; Raleigh, D. P.; Cruzet, F.; Griffin, R. G. *J. Chem. Phys.* **1990**, *92*, 6347.

(42) Kubo, A.; McDowell, C. A. *J. Chem. Soc., Faraday Trans. 1* **1988**, *84*, 3713.

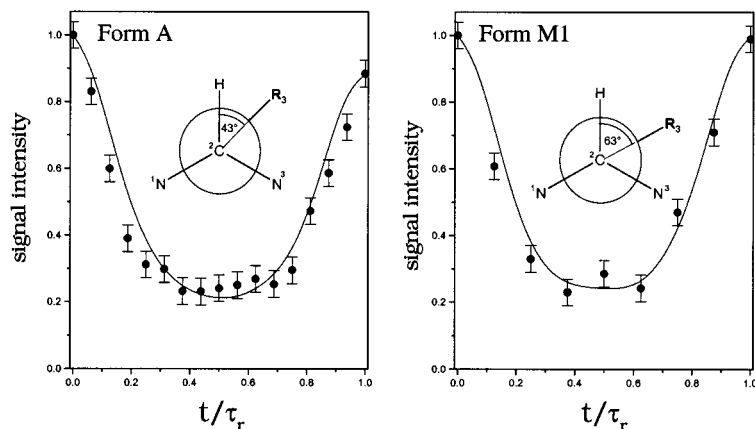


Figure 7. 2Q-HLF spectral amplitudes (filled circles) for [$^{13}\text{C}_2$]cimetidine form A (left) and form M1 (right). Error bars represent the standard deviation of the noise. In both cases the best-fitting simulations (solid lines) for the molecular conformations of form A ($r = 3.8 \text{ \AA}$; $\varphi = 108^\circ$; $\theta = 62^\circ$; $\phi = 43^\circ$) and form M1 ($r = 3.8 \text{ \AA}$; $\varphi = 114^\circ$; $\theta = 70^\circ$; $\phi = 63^\circ$) were obtained using a multiple pulse scaling factor κ of 0.27 and an H-C dipolar constant b^{HC} of 129 kHz.

The full rotational trajectory of the proton spin is expressed as N equal steps of duration Δt , and $\omega_{ji}^{\text{HC}}(t, i)$ is the local field calculated for the position of the C-H vector at each rotational step i , as defined by i sets of Euler angles $\Omega_{\text{PM}}(t_i)$. For cimetidine, $\alpha_{\text{PM}}(t_i)$, $\beta_{\text{PM}}(t_i)$, $\gamma_{\text{PM}}(t_i)$ are calculated from the angles ϕ , φ , and θ defined in Figure 2.

For a four-spin H-C-C-H system, the phase gained by the 2Q coherence after experiencing a local proton field for time t ($t \leq \tau_{\text{R}}$) during the evolution interval of the HLF experiment is described by phase angles for parallel and antiparallel proton spin polarizations, $\Phi^{\alpha\alpha}$ and $\Phi^{\alpha\beta}$ ³¹

$$\Phi^{m_1 m_2}(t) = 2\kappa \int_0^t (m_1 [\omega_{11}^{\text{HC}}(t) + \omega_{12}^{\text{HC}}(t)] + m_2 [\omega_{21}^{\text{HC}}(t) + \omega_{22}^{\text{HC}}(t)]) dt \quad (4)$$

The scaling factor κ takes into account the attenuation of the ^1H - ^{13}C dipolar interaction by the multiple pulses of MREV-8, and α and β are the shorthand notation for the quantum numbers $m = +1/2$ and $m = -1/2$. In the case of [$^{13}\text{C}_2$]cimetidine, with a remote, nonbonded ^{13}CH - $^{13}\text{CH}_3$ system, the methyl carbon spin experiences an equal, time-averaged local field from each of its three bonded protons, while the C-H carbon experiences a field from its single-bonded proton. Contributions from nonbonded protons can be neglected for cimetidine. Hence, the modulation of 2Q coherence is described by four phase angles, $\Phi^{\alpha 1}$, $\Phi^{\alpha 2}$, $\Phi^{\alpha 3}$, and $\Phi^{\alpha 4}$, corresponding to the proton polarizations in the effective field. The phase angles are derived from the local proton fields by combining each of the C-H spin-states with linear superpositions of the methyl proton spin-states,

$$\Phi^{\alpha 1} = 2\kappa \int_0^t \left(\frac{1}{2} \omega_{11}^{\text{HC}}(t) - \frac{3}{2} \omega_{22}^{\text{HC}}(t) \right) dt \quad (5a)$$

$$\Phi^{\alpha 2} = 2\kappa \int_0^t \left(\frac{1}{2} \omega_{11}^{\text{HC}}(t) - \frac{1}{2} \omega_{22}^{\text{HC}}(t) \right) dt \quad (5b)$$

$$\Phi^{\alpha 3} = 2\kappa \int_0^t \left(\frac{1}{2} \omega_{11}^{\text{HC}}(t) + \frac{1}{2} \omega_{22}^{\text{HC}}(t) \right) dt \quad (5c)$$

$$\Phi^{\alpha 4} = 2\kappa \int_0^t \left(\frac{1}{2} \omega_{11}^{\text{HC}}(t) + \frac{3}{2} \omega_{22}^{\text{HC}}(t) \right) dt \quad (5d)$$

The NMR signal amplitude a after MREV-8 homonuclear decoupling for time t is related directly to the modulation of 2Q coherences by local proton fields during homonuclear decoupling and is expressed as a combination of the four new

phase terms, as

$$a(t) = \langle \frac{1}{4} \sin^2(\omega_{2\text{Q}} \tau_{\text{exc}}) \exp(-T_2^{\text{DQ}}) \sum_{m=1}^4 \cos \Phi^{\alpha m}(t) \rangle \quad (6)$$

The terms $\omega_{2\text{Q}}$ and τ_{exc} are the double-quantum nutation frequency and C7 excitation time, respectively, defined in Lee et al.,³⁸ and T_2^{DQ} is the double-quantum relaxation time during the evolution period. In practice, the amplitudes a for cimetidine over one full rotor cycle were measured from the 2Q-HLF spectra obtained at 17 equally spaced values of t (e.g., Figure 3B) and numerical simulations were carried out using a number of input parameters (Figures 7 and 8). The important parameters in the calculation procedure are the proton-carbon dipole coupling constants b_{jk}^{HC} , the scaling factor κ , the double-quantum relaxation time, and the angles H-C2-C16 and R₃-C16-C2 (defined as θ and φ , respectively, in Figure 2) and the angle H-C2-C16-R₃ (defined as ϕ in Figure 2). The three angles partially define the molecular geometry of cimetidine, and combinations of values of these angles can be determined from the calculated amplitude curve giving the best fit to the experimental data, provided the remaining input parameters are known.

The simulations are complicated by uncertainties in the values of κ and in b_{jk}^{HC} . Single-crystal diffraction techniques can underestimate C-H bond lengths by a fraction of an angstrom owing to thermally induced molecular bond vibrations, which can lead to inaccuracies of as much as 15 kHz in the calculated ^{13}C - ^1H dipole coupling constants.³¹ Moreover, although a scaling-factor κ of 0.54 has been determined from calibrations on adamantane,⁴³ marked discrepancies from this value have been reported because of the sensitivity of κ experimental conditions. The values of κ and b_{jk}^{HC} are not affected by molecular conformation, however, and in the case of cimetidine, provided all 2Q-HLF experiments are conducted under the same conditions, the values should be identical or very similar for each form. The molecular geometry of forms A and M1 is known from their crystal structures, and b_{jk}^{HC} and κ are therefore the only unknown input parameters in the numerical simulation procedure. Simulations of the experimental amplitudes for form A and form M1 were carried out by systematically varying κ and b_{jk}^{HC} while keeping the known molecular geometric terms constant, to find the combination of values

(43) Terao, T.; Miura, H.; Saika, A. *J. Magn. Reson.* **1982**, *49*, 365.

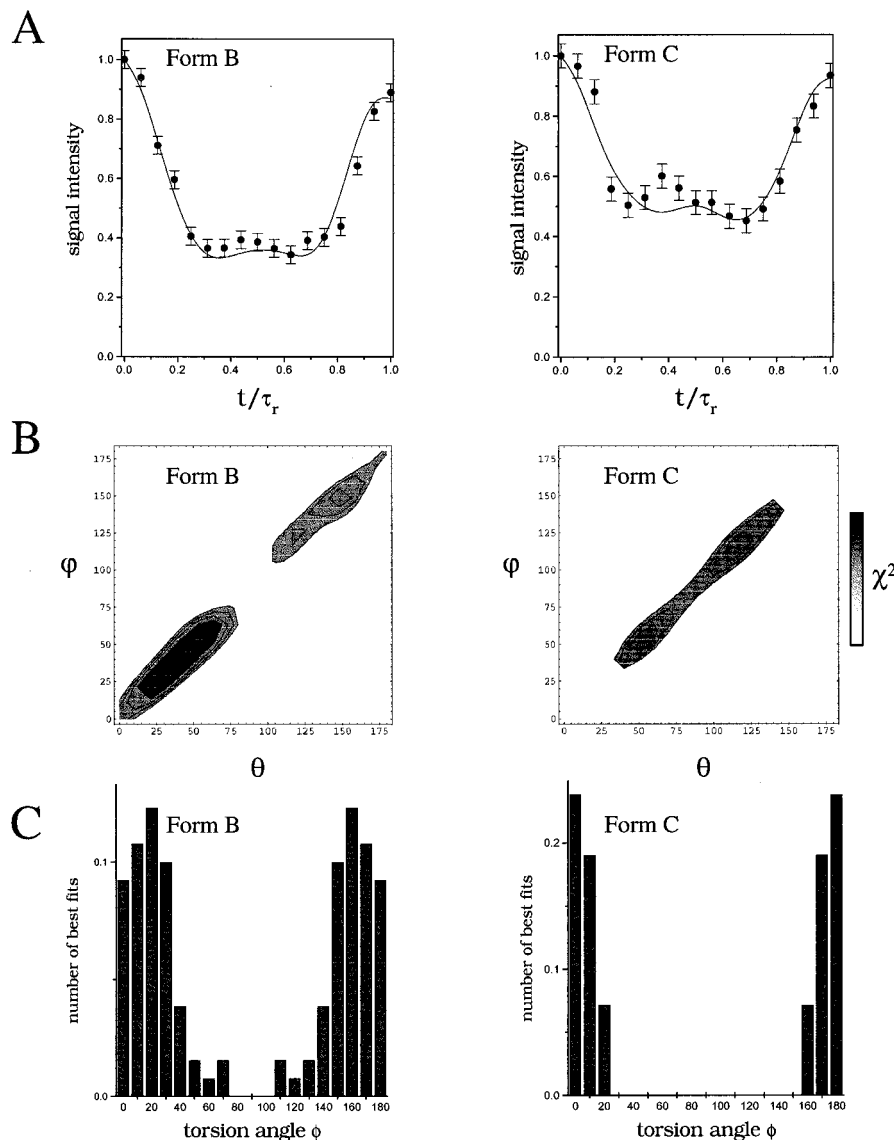


Figure 8. Illustration of the strategy for determining the conformationally diagnostic angles (φ , θ and ϕ) for cimetidine form B (left) and form C (right). (A) 2Q-HLF amplitudes over one rotor cycle (filled circles) were compared with curves calculated from the values of b^{HC} and κ given in Figure 7, and combinations of φ , θ and ϕ taking values from 0° to 180° . The solid lines are examples of simulations giving least-squares fits to the data. (B) Contour plots showing combinations of φ and θ values giving best-fitting simulations of the experimental data (dark regions represent χ^2 minima) when ϕ is fixed at 180° . (C) Relative numbers of φ/θ combinations giving best-fitting simulations of the experimental data, taken from 19 contour plots as in (B) in which angle ϕ was varied from 0° to 180° .

giving the least-squares fits to the experimental data (b_{11}^{HC} and b_{22}^{HC} were assumed to be identical). Input values of 129 kHz for b_{jk}^{HC} and 0.27 for κ provided the best-fitting simulations to amplitudes for both form A and form M1. These values were therefore used as fixed parameters in simulations of amplitudes for forms B and C, where the unknown geometric terms were the variable input parameters.

The experimental amplitude profiles for forms B and C were rather different in appearance from those of A and M1 (Figure 7). The efficiency of double-quantum excitation was much poorer for forms B and C (less than 1%) than for A and M1 (less than 10%) because of the greater separation and, consequently, smaller coupling between C2 and C16 in forms B and C than in A and M1. The 2Q amplitude profile is affected little by the magnitude of ^{13}C homonuclear dipolar coupling, however, and the distinction between the profiles of the different forms is attributable entirely to differences in the relative orientations of the ^{13}C – ^1H vectors. In the case of a directly bonded 4-spin system, such as in a segment of the side-chain of retinal, the

H–C–C bond angles are fixed (normally between 100° and 120°) and only the H–C–C–H torsion angle is variable. In cimetidine, however, C2 and C16 are not bonded to each other, and all three angles are variable, according to molecular conformation, taking values from 0° to 360° (Figure 2). Numerical simulations of the 2Q-HLF data for forms B and C therefore involved computation of curves for the entire range of possible values of angles ϕ , φ , and θ , while keeping all other input parameters constant, to find the least-squares fits to the experimental data (Figure 8).

The contour graphs in Figure 8 show χ^2 values obtained by comparing the experimental amplitude profiles for forms B and C with curves computed by fixing angle ϕ at 180° and varying angles θ and φ from 0° to 180° . A set of 19 contour graphs of this type was produced for values of angles ϕ of 0° , 10° , 20° ... 180° . The dark contours show the combinations of angles giving acceptable fits to the experimental data. The area of the dark contours in each of the 19 graphs are plotted against angle ϕ (Figure 8; middle) to illustrate the number of θ/φ combinations

at each angle ϕ that are consistent with the experimental data. For form B, the experimental amplitude profiles are consistent with a number of θ/φ combinations for all values of ϕ outside the range 80–100°. The experimental profiles for form C, however, were consistent with a much smaller range of ϕ values, restricted to between 0° and 20° and 160° and 180°.

Computation of Cimetidine Conformations. Rotational resonance distance measurements gave a qualitative impression of how the molecular conformations of cimetidine in the structurally undefined forms B and C compared with the crystal structures of forms A, D, and M1. The bent conformations of cimetidine in forms A and M1 (Figure 1) give rise to a short C2–C16 interatomic distance of less than 4 Å, and in form D the molecule adopts an extended conformation with a distance of over 9 Å (Figure 1). The distance range measured for forms B and C was 5.5 ± 0.3 Å in both cases, indicating that the molecular conformations in these crystal forms lie between the extended and bent extremes.

A simple computational method was devised to search the conformational space of cimetidine for possible structures of forms B and C that were consistent with rotational resonance distance measurements and with the angles determined in the 2Q-HLF experiment. The computational approach was carried out as follows. First, atomic coordinates in an arbitrary reference frame were calculated for molecular conformations of cimetidine covering its entire structure space, derived by rotating each of the seven rotationally labile bonds through 360° in 30° increments. The number of possible structures in the search space exceeded 3×10^7 , but combinations of angles that would clearly produce high-energy structures (such as adjacent torsional angles of $<20^\circ$) were not included in the calculations to reduce computation time. The computationally generated coordinates were then scanned for structures having overlapping bonds or atomic radii, and the unfeasible structures were eliminated from the subsequent analysis.

The next step of the procedure was to compare the remaining coordinates with the experimental data for forms B and C. The C2–C16 distance was calculated for each of the remaining coordinates in the data set, and only those coordinates in which the distance lay between 5.2 and 5.8 Å, the distance range determined by rotational resonance for forms B and C, were selected. At this stage the number of structures in agreement with the experimental data had been reduced to about 5000. To lower this number further, the angles ϕ , φ , and θ defining the relative orientations of the C–H bonds in the guanidinium and imidazolium groups were used as additional restraints on the molecular conformations of forms B and C.

In the case of form B, the large number of possible angle combinations (Table 1), which included almost the entire range of permitted values of ϕ , precluded the possibility of the true molecular structure being determined unambiguously from the existing experimental restraints. In fact, the number of cimetidine structures from the remaining data set, which were consistent with the combined distance and angle measurements obtained for form B, remained higher than 1000. An additional complication arises from the fact that at least two crystallographically nonequivalent molecules occupy the unit cell of form B, and it is therefore not known if the individual molecules differ in their three-dimensional structures as well as in their spatial relationship to each other. Hence, it is possible that the geometric measurements for form B are population-averaged values representing two or more conformations of cimetidine in the unit cell. Consequently, further NMR experiments involving

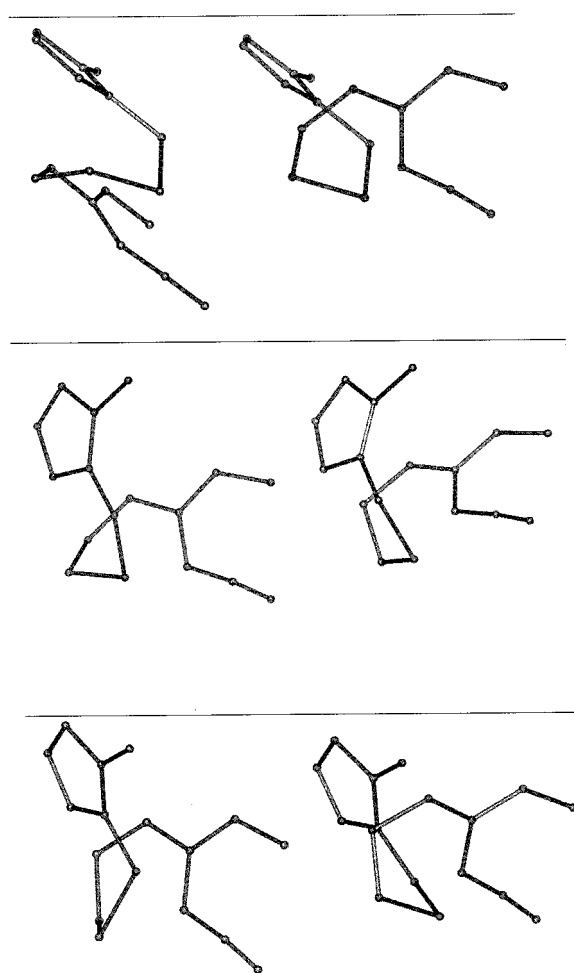


Figure 9. Representative molecular conformations of cimetidine from each of six groups consistent with the C2–C16 distance (5.2–5.8 Å) and relative C–H orientations measured from form C by rotational resonance and 2Q-HLF NMR. Mirror images conformations are also feasible but are not shown.

alternative isotope labeling schemes will be necessary to gain more insight into the structure of cimetidine form B.

The angle measurements obtained for cimetidine form C were more favorable for reducing significantly the molecular conformations in the data set that were close or identical to the true structure of cimetidine in this crystal form. In form C only one molecule constitutes the crystallographic asymmetric unit, eliminating ambiguities arising from conformational heterogeneity in the crystal lattice, and far fewer combinations of angles φ , θ , and ϕ are consistent with the 2Q-HLF amplitudes than were found for form B (Table 1). After comparing the 5000 cimetidine structure coordinates remaining in the data set with the measured geometric terms for form C, fewer than 200 structures were found to be consistent with the combinations of φ , θ , and ϕ .

In the final step, nonbond (van der Waals and electrostatic) interaction energies were calculated using the Biosym/MSI package Insight II for the few remaining structures in the data set derived from the experimental data for form C. In so doing, a number of energetically similar cimetidine conformations were identified having significantly lower interaction energies (by <100 kcal/mol) than those of other conformations in the data set. These minimum-energy conformations could be separated into groups: each group consisted of 6–12 closely related conformations in which the seven torsional angles fell within a 60° range. Only 12 such groups were identified using this

approach (Figure 9), but because the 2Q-HLF experiment is unable to distinguish between positive and negative angles, the groups could be separated further into six pairs of mirror images. The restricted search space used for identifying these molecular conformations was defined by rotation of the seven cimetidine bonds in 30° increments, and errors of $\pm 15^\circ$ must therefore be placed on each of the torsion angles defining the molecular structures in the final structure groups.

This combined approach identified a manageable number of cimetidine structures (Figure 9), from which it may be possible to determine the true structure of form C using molecular dynamics and simulated annealing procedures (Figure 9). Although sophisticated structural refinement approaches are beyond the scope of the present work, it is possible at this stage to identify for the first time some structural features of cimetidine that are present in form C. The predominant feature in all the structures identified in Figure 9 is a twisted "corkscrew" conformation around the sulfide linkage, which, because of the planar configuration of the guanidinium moiety, might allow intramolecular hydrogen bonding between the guanidinium NH proton and the imidazolium nitrogen. Other spectroscopic techniques, such as resonance Raman and FT-IR may help to shed light on the hydrogen bonding characteristics in this cimetidine form.

Conclusions

This work has demonstrated a strategy that uses a combination of isotope labeling, solid-state NMR spectroscopy, and computational analysis to investigate the structures of polycrystalline compounds in the absence of diffraction techniques. The

approach is shown to be useful in structural studies of polymorphic materials, particularly in cases where the crystal structures of some crystalline forms of a compound have been solved but others have not. The attractive feature of this approach is that a large amount of structural information, more than a single distance measurement, can be obtained by solid-state NMR without uniformly labeling the compounds, which is advantageous for minimizing expenditure and for reducing the need to develop novel synthetic routes. The disadvantage of the approach is that the information provided from the distance and angle measurements may be ambiguous, and it cannot always be determined a priori if a unique structure of a compound can be identified without additional NMR measurements or computational refinement. Nevertheless, it is envisaged that this NMR strategy could play a valuable and economical role in solid-state structural chemistry if it is used to support other techniques, such as computational statistical methods for structure determination from synchrotron powder diffraction patterns.⁴⁴

Acknowledgment. We thank Malcolm Levitt and Clemens Glaubitz for providing rotational resonance simulation programs, Xialong Feng for kindly supplying a copy of his Doctorate thesis containing the theoretical treatment of 2Q-HLF, and Frederic Berst for assistance with cimetidine crystallization. Part of this work was carried out at the National Biological Solid State NMR Facility, Harwell, U.K.

JA993067Z

(44) Wessels, T.; Baerlocher, C.; McClusker, L. B. *Science* **1999**, *284*, 477.